Underlying mechanism of Qiling Jiaogulan Powder in the treatment of broiler ascites syndrome

Juan Yu,* Xingyou Liu,† Keyao Wang,* Huimin Wang,* Yufeng Han,* Jie Kang,* Ruiqiang Deng,* Huaijun Zhou,* and Zhibian Duan*,[1]

*College of Veterinary Medicine, Shanxi Agricultural University, Taigu, Shanxi, 030800, China; and †School of Life Science and Basic Medicine, Xinxiang University, Xinxiang, Henan, 453003, China

ABSTRACT Broiler ascites syndrome (**AS**), is a nutritional and metabolic disease that occurs in fast-growing commercial broiler chickens. AS can cause poor growth and a significant increase in the rate of broiler deaths, which has resulted in serious economic losses to the poultry industry. The classic traditional Chinese medicine Qiling Jiaogulan Powder (**QLJP**) has been demonstrated to have a certain therapeutic effect on broiler AS. However, its pharmacological mechanism remains to be elucidated. This study was performed to investigate the multitarget action mechanism of QLJP in the treatment of broiler AS based on network pharmacology analysis using a broiler AS model. First, all chemical components and targets of QLJP were obtained from the Traditional Chinese Medicine System Pharmacology Analysis Platform (**TCMSP**). Targets related to broiler AS were further obtained through the GeneCards database and the NCBI Gene sub-database. A protein−protein interaction (**PPI**) network was constructed. Then, enrichment analyses were performed to predict the potential mechanisms of QLJP in the treatment of broiler AS. Finally, the treatment effect of QLJP on AS was verified in a broiler AS model. Network pharmacology analysis generated 49 active ingredients and 167 core targets of QLJP, and a QLJP−single drug−target−disease network was successfully constructed. Gene enrichment analysis indicated that the core targets have played major roles in the Cell cycle, FOXO signaling pathways, etc. We demonstrated that QLJP improved clinical and organ damage symptoms and significantly reduced the ascites heart index in broilers with AS induced by administration of high-energy, high-protein diets and high-sodium drinking water in a low-temperature environment. QLJP may regulate lung oxidative stress, the cell cycle and apoptosis by activating the FOXO3a signaling pathway to interfere with the occurrence and development of AS in broilers. QLJP administration may be a good clinical strategy for the prevention and treatment of broiler AS.

Key words: broiler ascites syndrome, Qiling Jiaogulan Powder, mechanism, network pharmacology, FOXO3a signaling pathway

2023 Poultry Science 102:102144
https://doi.org/10.1016/j.psj.2022.102144

INTRODUCTION

Broiler ascites syndrome (**AS**), also known as broiler pulmonary hypertension syndrome (**PHS**), is a nutritional metabolic disease that occurs in fast-growing commercial broilers (Kalmar et al., 2013). This disease can cause massive economic losses to the poultry industry worldwide (Wideman et al., 2011). Studies have found that low temperature and high-energy, high-protein, and high-sodium diets, which can increase the metabolic rate and tissue oxygen consumption of broilers, resulting in relatively hypoxic in broilers (Julian, 1993; Wideman et al., 2013). Hypoxia in broilers causes some symptoms such as tissue oxygen free radical damage, increased cardiac output, insufficient pulmonary blood volume, right heart hypertrophy, and pulmonary arterial hypertension. Indeed, Pulmonary arterial hypertension (**PAH**) is the central event in the onset of broiler AS. The continuous development of PAH leads to comprehensive pathophysiological changes such as increased tissue oxidative stress damage, pulmonary vascular remodeling, right heart failure and ascites (Humbert et al., 2004). The main pathological feature of PAH is vasoconstriction, excessive cell proliferation, apoptosis resistance, and increased deposition of extracellular matrix components, which contributes to increase pulmonary vascular resistance and decreased compliance (Bordenave et al.,

Received January 22, 2022.
Accepted August 19, 2022.

[1]Corresponding author: duanzhibian@163.com

2019). It has been reported that hypoxia is the basis of the pathogenesis of lung diseases, causing damage or dysfunction of the pulmonary endothelium, which abnormally secretes inflammatory factors, growth factors and vasoactive factors, etc. Then these factors induces increased cell proliferation and apoptosis resistance in pulmonary arteries, and abnormal synthesis of extracellular matrix, lead to increasing pulmonary artery remodeling, ultimately leading to the occurrence of PAH (Stenmark et al., 2006; Tuder et al., 2007). It has been proved that the balance between cell proliferation and apoptosis is an important mechanism for maintaining the integrity of organ functions (Courboulin et al., 2012). All these findings prove that cell proliferation and apoptosis play important roles in PAH, which is of great significance for screening drugs to treat AS in broilers.

Traditional Chinese Medicine has been used in the diagnosis and pathophysiological treatment of diseases for thousands of years (Xu et al., 2013). At present, Traditional Chinese Medicine is widely used in the treatment of broiler AS (Shi et al., 2005; Qi and Wang, 2006; Dai et al., 2007). QLJP is a classic traditional Chinese medicine compound in the Veterinary pharmacopoeia, which is composed of *Astragalus membranaceus, Poria cocos, Arnebia euchroma, Gynostemma pentaphyllum*, and *Alisma orientale. Astragalus membranaceus* has the ability to inhibit cell proliferation, induce apoptosis, cell cycle arrest and decrease metastasis, thereby exerting a wide range of pharmacological effects such as anti-inflammatory, antioxidant, and inhibiting pulmonary hypertension (Hu et al., 2009; Fu et al., 2014; Wang et al., 2021). *Poria cocos* has important pharmacological activities in anti-inflammatory, antioxidant, cell cycle arrest and apoptosis (Ríos, 2011; Zhao et al., 2020). Shikonin is one of the main active ingredients of *Arnebia euchroma*, which can significantly inhibit the expression of Cyclins D1 and E, promote the expression of p21, and has a clear effect on anti-proliferation, promoting apoptosis and blocking cell cycle progression of VSMC (Zhang et al., 2005). *Gynostemma pentaphyllum* has a wide range of pharmacological effects in clinical applications, including antioxidant (Li et al., 2015), cell cycle arrest (Tsui et al., 2014; Zhang et al., 2015), antiproliferation and induction of apoptosis (Wang et al., 2007; Cheng, et al., 2011). In addition, Studies have confirmed that *Alisma orientale* has the pharmacological effects of anti-inflammatory, inducing cell cycle arrest and apoptosis (Wei et al., 2018; Feng et al., 2021). However, the active ingredients and pharmacological mechanism of QLJP remains to be elucidated.

Network pharmacology combines the field of systems biology with pharmacokinetic and pharmacodynamic properties to study drugs, protein targets, and pharmacological activities in order to explore how drugs work (Liu et al., 2015). Network pharmacology is based on drug−gene−target−disease interaction networks and systematically provides information on the effects of drugs on some diseases (Zhang et al., 2019). This approach is in line with the theory of traditional Chinese medicine, which emphasizes the diagnosis and treatment of diseases from a holistic perspective and takes advantage of the synergy between Chinese herbs and their compounds (Yuan et al., 2017). In this study, we first used network pharmacology methods to analyze the active ingredients of QLJP and their potential targets and pathways and clarified the synergistic effects and mechanism of QLJP, and preliminarily screened the FOXO signaling pathway.

Forkhead box O3 (**FOXO3a**), an important transcriptional regulator in the FOXO subfamily, is an important regulator of cell differentiation, metabolism, follicle maturation, cell proliferation, apoptosis, DNA damage repair, and oxidative stress in mammalian cells (Brown and Webb, 2018; Tia et al., 2018). FOXO3a is activated by posttranslational modifications, after which it can induce the expression of downstream target genes, including antioxidant genes, apoptosis and cell cycle genes, and exert a variety of biological effects (Wang et al., 2016). Studies have found that FOXO3a can enhance the ability of cells to resist oxidative stress under hypoxic conditions (Li et al., 2010; Reiterer and Milton, 2020). In addition, FOXO3a has been found to inhibit VSMC proliferation, endothelial cell migration, cardiomyocyte proliferation and hypertrophy, and antioxidative stress in rat experiments (Papanicolaou et al., 2008). Other study also showed that the regulation of FOXO3a signaling pathway is a potential new therapeutic mechanism for anti-hypertensive vascular remodeling and protection of target organs (Chung et al., 2012). We speculated that FOXO3a signaling pathway may play a regulatory role in the pathogenesis of broiler AS. Therefore, based on the network pharmacology analysis, we conducted an animal experiment to verify the mechanism of QLJP in the treatment of AS in broilers via the FOXO3a signaling pathway.

MATERIALS AND METHODS

Screening of Bioactive Compounds in QLJP and Disease Target Prediction

The compounds and compound-related targets of QLJP were collected from the Traditional Chinese Medicine Systems Pharmacology database (http://tcmspw.com/tcmsp.php). Oral bioavailability (**OB**) and drug-likeness (**DL**) are commonly used parameters for screening of active compounds in herbs. The compounds of QLJP were searched in the TCMSP database, and compounds with OB $\geq$ 30% and DL $\geq$ 0.18 were selected as the active compounds of QLJP. According to the "related targets" function in the TCMSP database, the targets corresponding to the compounds were retrieved, and the target protein names were uniformly converted into gene names using the UniProt database (https://www.uniprot.org/). In addition, a QLJP−single drug−compound−target network was constructed with Cytoscape 3.6.1 software. Broiler AS-related genes were collected from two databases, namely, the GeneCards database and the NCBI Gene sub-database.

Protein−protein Interaction (PPI) Network Construction

The complex interrelationships between drugs and diseases can be clarified through visualization of protein interaction networks and drug−active ingredient−target−disease networks. Drug active compounds can directly or indirectly act on disease targets to exert therapeutic effects, and the formation and treatment of diseases are also directly or indirectly related to their targets. The BisoGenet plugin of Cytoscape 3.6.1 was used to construct a drug−compound−target PPI network and a disease−target PPI network. The Merge function was used to merge the 2 PPI networks and extract the intersecting network in order to obtain the direct and indirect targets of QLJP in the treatment of broiler AS. The CytoNCA plugin of Cytoscape was used to screen the core targets of QLJP in the treatment of broiler AS, and a QLJP−single drug−target−disease network was constructed.

Gene Ontology (GO) and Kyoto Encyclopedia of Genes and Genomes (KEGG) Pathway Enrichment Analysis

GO enrichment analysis is often used to annotate the functions of genes and their gene products. It includes three biological categories, namely, the molecular function (**MF**), biological process (**BP**), and cellular component (**CC**) categories. The KEGG can be used to conduct pathway enrichment analysis of targets, which is helpful for exploring the mechanisms of drugs in the treatment of diseases. In this study, the OmicShare database was used to perform GO functional and KEGG pathway enrichment analyses on the screened core targets in order to elucidate the potential gene functions and signaling pathways of the targets of the active ingredients in QLJP through which QLJP helps treat broiler AS.

Animal Experiment Design

All experiments were approved and conducted in accordance with the guidelines of the Animal Ethics Committee of Shanxi Agricultural University. The components of QLJP were radix astragalus (*Astragalus membranaceus* (Fisch.) Bunge., Huangqi), poria (*Poria cocos* (Schw.) Wolf., Fuling), radix arnebiae (*Arnebia euchroma* (Royle) Johnst., Zicao), herba gynostemmae (*Gynostemma pentaphyllum* (Thunb.) Makino., Jiaogulan), and rhizoma alismatis (*Alisma orientale* (Sam.) Juzep., Zexie) (all purchased from Taigu County Medicinal Materials Company, Shanxi, Taigu, China). The 5 traditional Chinese herbs were pulverized into powder, sieved, and mixed in a ratio of 4:7:3:3:3 to obtain QLJP, and the dosage of QLJP used in this experiment was referred to the Veterinary Pharmacopoeia of the People's Republic of China (Chinese Veterinary Pharmacopoeia Committee, 2017). One hundred and fifty 1-day-old Ross 308 broilers (37−42 g) and a standard diet were purchased from Shanxi Wenshui Elephant Poultry Co., Ltd. (Shanxi, Taigu, China). After 7 d of adaptive feeding, the birds were divided into 6 groups: the control group (20 birds); the model group (26 birds); the L-arginine (L-Arg) group (26 birds); and QLJP low-, medium-, and high-dose groups (26 birds of each group). The broilers were allowed to drink and eat freely. All broilers in the control group were given a regular diet and tap water in an environment of 22 to 25°C. Those in other groups were provided with a high-calorie diet (supplemented with 3% lard and 4% fish meal), a water with 0.12% salt, and a low temperature of 9 to 11°C to induce broiler AS. In addition, the broilers in the L-Arg group received a diet mixed with 1% L-arginine (Ahmadipour et al., 2018). Each QLJP group was fed a diet mixed with QLJP (high, medium, and low: 0.4%, 0.2%, and 0.1%).

At 21, 28, 35, and 42 d of age, 5 broilers were randomly selected from each group and weighed, and changes were observed by clinical examination and necropsy. The chest cavity was opened, and the lungs and heart were quickly and completely removed. The ascites heart index (**AHI**) was examined, and a small piece of lung tissue was cut, quickly placed in liquid nitrogen and then transferred to a −80°C freezer for storage.

The clinical symptoms of broilers with AS included cyanosis of the wattles and skin, reduced weight, and an enlarged abdomen with fluctuating size. The signs of AS on necropsy included a large amount of yellow clear fluid in the abdominal cavity, pericardial effusion, liver congestion and enlargement, a yellow jelly like substance on the liver surface, and an ascites volume greater than 20 mL. The onset of AS was determined based on the above symptoms, and the AHI >0.25 is another index to judge the occurrence of broiler AS (Julian et al., 1989). The right ventricle was cut away from the left ventricle and septum, the RV and TV were recorded. The AHI was calculated as the ratio of the right ventricular weight (**RV**) to the total ventricular weight (**TV**) (Julian, 1987).

Observation of Lung Histopathology

Fresh lung tissue was cross-sectioned along the left hilum and fixed with 4% paraformaldehyde. According to the conventional paraffin section method, the lungs were cut into slices with a thickness of approximately 5 μm and stained with hematoxylin-eosin to observe the pathological changes in the lungs (microscope model: Nikon Eclipse ci, imaging system: Nikon DS-FI2).

Estimation of the Oxidation/Antioxidation Index

Next, 0.1 g of each lung tested was used to prepare a 10% tissue homogenate using a low-temperature homogenizer. Then, the tissue homogenate was centrifuged at 2500 rpm for 10 min at 4°C, and the supernatant was

taken for index detection. The double antibody sandwich method was used to detect the levels of lung oxidation/antioxidation indicators with a chicken superoxide dismutase (**SOD**) ELISA kit, a chicken glutathione peroxidase (**GSH-Px**) ELISA kit, a chicken catalase (**CAT**) ELISA kit, and a chicken malondialdehyde (**MDA**) ELISA kit (Shanghai Enzyme-linked Biotechnology Co., Ltd, Shanghai, China) according to the instructions.

Real-time Fluorescence Quantitative PCR Detection of Broiler Lung Tissue

The lung samples were washed with prefrozen diethyl pyrocarbonate water, immediately frozen in liquid nitrogen and stored at −80°C. Approximately 100 mg of each preserved sample was ground thoroughly with liquid nitrogen in a precooled mortar. Total RNA was extracted with TRIzol (Invitrogen, Carlsbad, CA). The RNA concentration was determined, and RNA with a D260/D280 ratio of 1.8 to 2.0 was used for reverse transcription. Then, reverse transcription was performed with a PrimeScript RT Reagent Kit with gDNA Eraser (TaKaRa, Dalian, China) according to the manufacturer's instructions. Real-time fluorescent quantitative PCR was used to detect *FOXO3a*, Tumor Protein P53 (***TP53***), B cell lymphoma/leukemia 2 (***BCL2***), Cyclin-dependent kinase 2 (***CDK2***) and CyclinD1 (***CCND1***) gene expression levels, with *β-actin* as the internal reference, with a SYBR Green Remix Ex Taq kit (TaKaRa, Dalian, China) according to the manufacturer's instructions. The $2^{-\Delta\Delta Ct}$ method was used for relative quantitative analysis of the data, and the relative expression of the target genes in each sample was calculated.

Immunohistochemical Detection of FOXO3a Protein Expression in the Lungs

An immunohistochemical assay was performed with a FOXO3a polyclonal primary antibody (LSBio, Seattle, WA), an HRP goat anti-rabbit IgG secondary antibody and a DAB color reagent kit (ZSGB-BIO, Beijing, China). A FOXO3a immunohistochemical assay was performed on lung tissue according to a standard procedure. Under the microscope, a brownish-yellow color was observed on the sites with positive expression of FOXO3a. Image-Pro Plus 6.0 image analysis software was used to determine the average optical density (**AOD**) of FOXO3a-positive cells, and the AOD value represents the protein expression of FOXO3a. A total of 10 fields of view were randomly selected and assessed. Their average value was used as the representative value of the section.

Detection of TP53, BCL2, CDK2, and CCND1 Protein Levels in the Lungs

Lung tissue (0.1 g) was added to 100 μL of precooled PBS (pH 7.4), and a tissue homogenate was prepared by using a low-temperature homogenizer. The homogenate was centrifuged at 3,000 rpm for 20 min at 4°C, and the supernatant was collected for detection. According to the instructions of a chicken Tumor protein p53 (**TP53**) ELISA kit, a chicken B cell leukemia/lymphoma 2 (**BCL2**) ELISA kit, a chicken Cyclin-dependent kinase 2 (**CDK2**) ELISA kit, and a chicken CyclinD1 (**CCND1**) ELISA kit, the double antibody sandwich method was used to detect the protein levels of TP53, BCL2, CDK2, and CCND1 (Shanghai Enzyme-linked Biotechnology Co., Ltd, Shanghai, China).

Statistical Analysis

All data were expressed as the mean ± SEM. One-way ANOVA was performed using statistical software SPSS 23.0. Differences was considered statistically significant at $P < 0.05$ or $P < 0.01$. Asterisks represented that these differences between the control group and the model group were statistical significance, and pound signs signified that the values were statistically different between the model group and the QLJP groups, L-Arg group ($^{*}P < 0.05$, $^{**}P < 0.01$; $^{\#}P < 0.05$, $^{\#\#}P < 0.01$).

RESULTS

QLJP−Single Drug−Compound−Target Network Construction

Compounds without corresponding targets, duplicates and target proteins without corresponding gene names were eliminated, and a total of 49 active compounds were identified in QLJP from the TCMSP database according to the screening conditions. The active compounds according to the degree value are listed in Supplementary Table 1. Sixteen compounds were found in *Astragalus membranaceus*, 6 compounds were found in *Poria cocos*, 11 compounds were found in *Arnebia euchroma*, 13 compounds were found in *Gynostemma pentaphyllum*, and 7 compounds were found in *Alisma orientale*. In addition, 196 potential targets corresponding to the active compounds of QLJP were obtained. The numbers of targets differed for the different compounds, and the targets overlapped significantly. A QLJP−single drug−compound−target network was constructed (Figure 1). In this network, we found that 172 targets were connected to at least two compound molecules, and approximately 87.8% of proteins shared common ligands with other proteins. Moreover, most of the active compounds in the network were connected to at least two targets, which also indicated that the active compound molecules in QLJP may coordinate with each other to act on the entire biological network. These results reflect the mechanism of mutual action among the multiple components and multiple targets of QLJP, which is also consistent with the general characteristics of traditional Chinese medicine compound prescriptions.

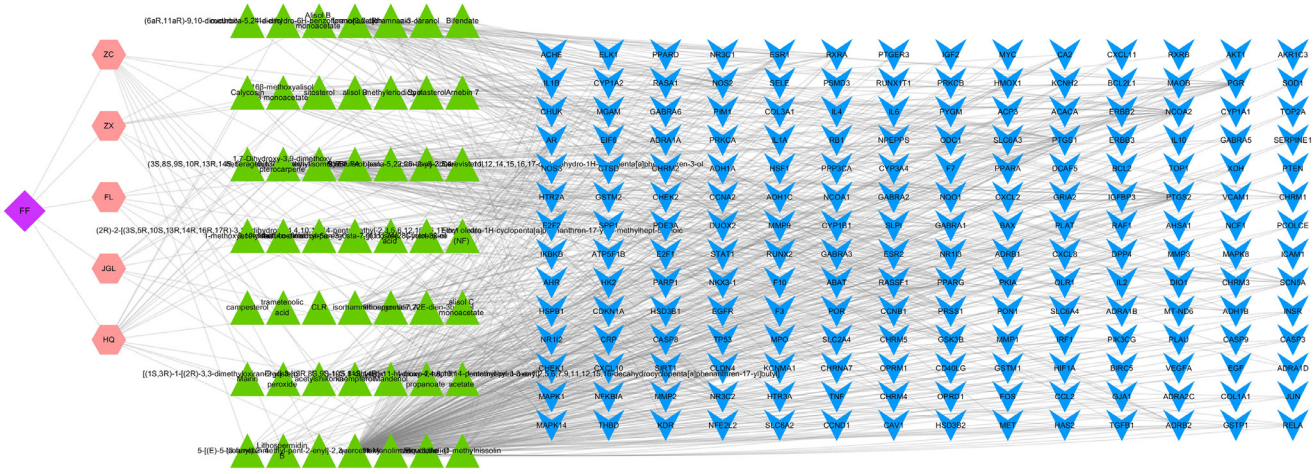

Figure 1. QLJP−single drug−compound−target network. Purple rhomboid node represent QLJP, Orange hexagon nodes represent Chinese Herbs, Green triangle nodes represent active compound, Blue figure nodes represent targets.

PPI Network Construction and Analysis

Using "ascites syndrome" and "broilers" as keywords for searching and screening, a total of 72 target genes closely related to AS were obtained, of which 68 and 4 related targets were retrieved from the GeneCards and Gene databases, respectively. A PPI network of QLJP potential targets and AS targets was constructed through the Merge function of Cytoscape, and 1,865 targets were obtained with 42,930 relationships (Figure 2A). The CytoNCA plugin was used to analyze the network. The nodes with the most connected targets were considered potential key targets. The targets for QLJP in the treatment of broiler AS were screened using parameters such as the degree value, medium degree, and tightness. The initial screening was based on a degree value ≥60. The QLJP−target−disease protein interaction network was then developed, and 467 targets were obtained with 16,681 interrelationships among the targets (Figure 2B). In the second screening, a degree value ≥95, a betweenness ≥3,732.7, and a closeness ≥0.32 were used to select core targets for QLJP in the treatment of AS in broiler, and 167 targets were obtained, with 4,256 interrelationships among targets (Figure 2C). Then, a QLJP−single drug−target−disease network was successfully constructed (Figure 3). According to the relationship between the core targets and the single drugs in QLJP, *Astragalus membranaceus* had the strongest effects on the core targets, playing major roles in combating AS in broilers. There was significant target overlap among the single herbs, which suggests that the five herbs in QLJP may have a synergistic effect.

GO Function Analysis and KEGG Enrichment Analysis

GO functional enrichment for the 167 core targets resulted in the identification of 117 BP terms, which mainly included the positive regulation of fibroblast proliferation, positive regulation of transcription from RNA polymerase II promoter, positive regulation of transcription, DNA templates, DNA repair, negative regulation of the cell cycle, regulation of apoptotic process, negative regulation of smooth muscle cell proliferation, negative regulation of cell proliferation, regulation of endothelial cell proliferation, response to hypoxia, positive regulation of nitric oxide biosynthetic process, inflammatory responses and cellular response to lipopolysaccharide terms. There were enriched 37 terms in the MF category; these terms were mainly related to damaged DNA

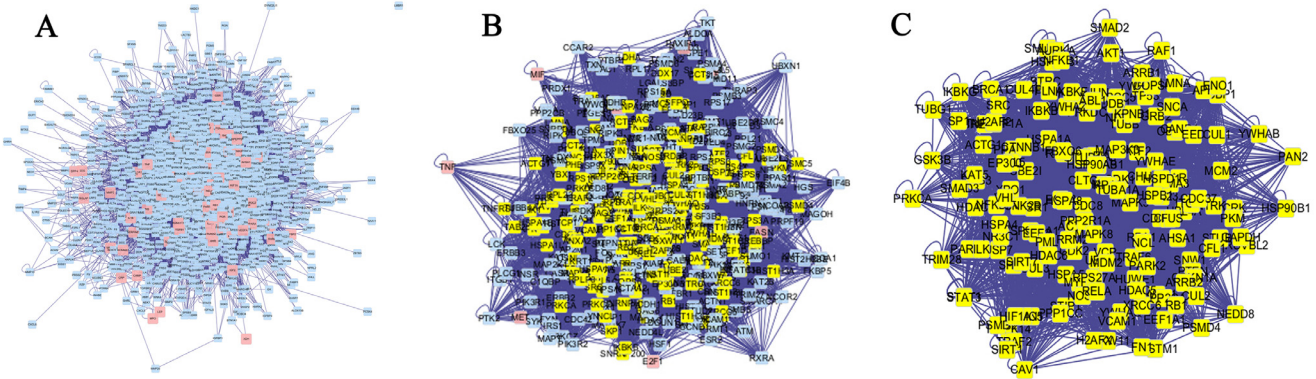

Figure 2. Drug-target-disease interaction network. (A) PPI network of QLJP and broiler AS. (B) QLJP−target−disease protein interaction network. (C) Core targets of QLJP in the treatment of broilers AS.

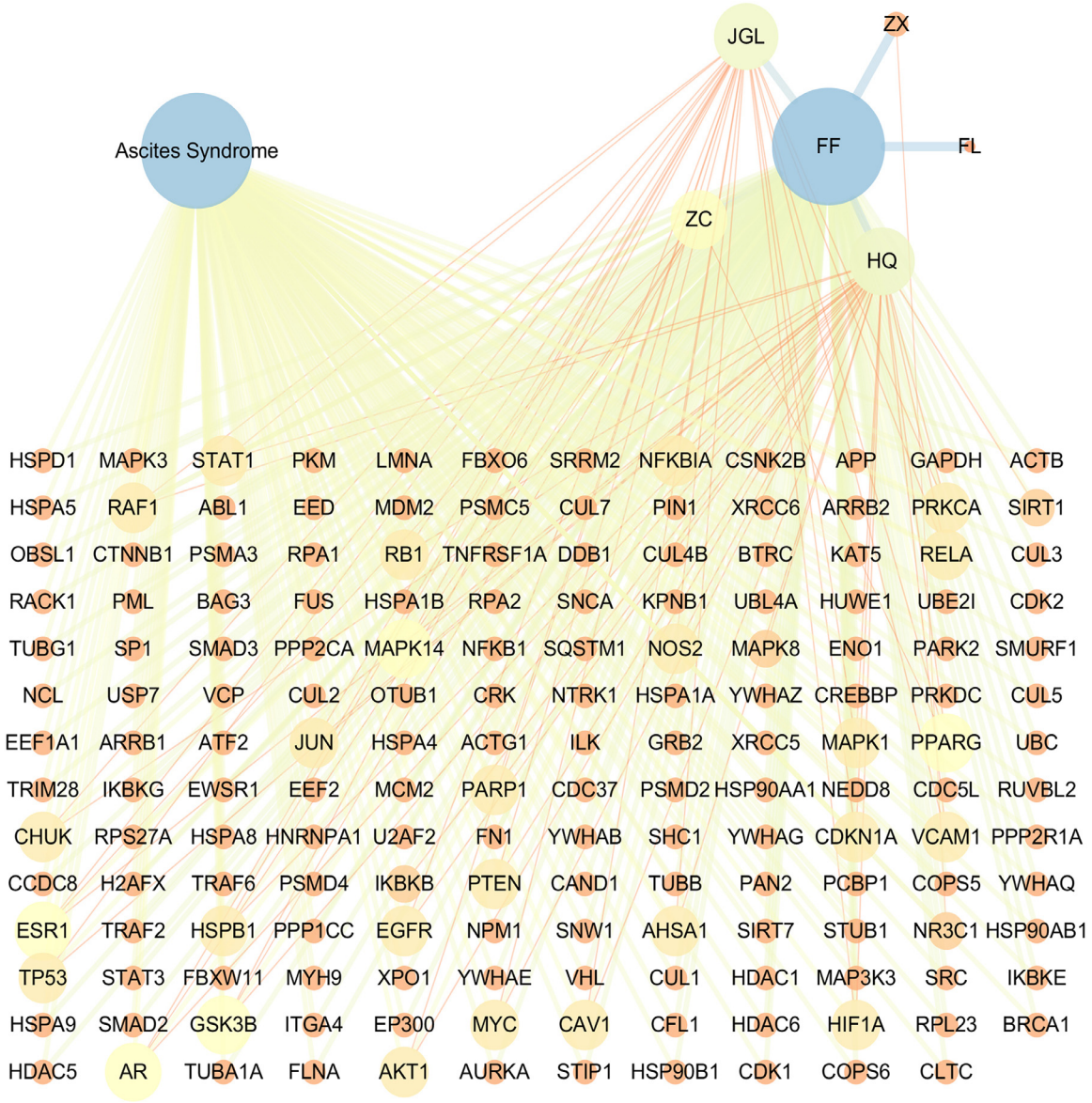

Figure 3. QLJP−single drug−target−disease network. FF: Qiling Jiaogulan Powder, HQ: *Astragalus membranaceus*, JGL: *Gynostemma pentaphyllum*, FL: *Poria cocos*, ZX: *Alisma orientale*, ZC: *Arnebia euchroma*.

binding, protein binding, transcription factor binding, transcription factor activity, TPR domain binding, nitric oxide synthase regulating enzyme activity, ATP binding, and poly(A) RNA binding. In addition, there were 15 terms in the CC category; these terms were mainly related to exosomes, nuclei, cell components, and cytoplasmic membranes.

Further KEGG enrichment analysis identified 35 signaling pathway terms, including the Cell cycle, FOXO signaling pathway, Adherens junction, Regulation of actin cytoskeleton, Focal adhesion, MAPK signaling pathway, Apoptosis, TGF-β signaling pathway, ErbB signaling pathway, Wnt signaling pathway, NOD-like receptor signaling pathway, Toll-like receptor signaling pathway, Insulin signaling pathway, VEGF signaling pathway, and P53 signaling pathway, etc. These signaling pathways play important roles in the mechanisms of the active compounds in QLJP for the treatment of broiler AS.

OmicShare was used to visualize the top 20 GO terms and the top 10 KEGG pathways (Figure 4) (https://www.omicshare.com/).

Effect of QLJP on Clinical Necropsy Changes in Broilers

The onset of AS was determined based on the clinical symptoms of broiler chickens, changes in necropsy phenotypes, and ascites volumes. The results showed that compared to those of the control group, the broilers of the model group were lighter, with disheveled feathers and enlarged abdomens. At the later stage of the trial, the broilers of the model group had cyanosis; shortness of breath; soft, fluctuating abdomens; and 50 to 200 mL of clear yellow liquid. Necropsy showed pericardial effusion, ventricular hypertrophy, liver congestion and swelling with a jellylike substance attached to the

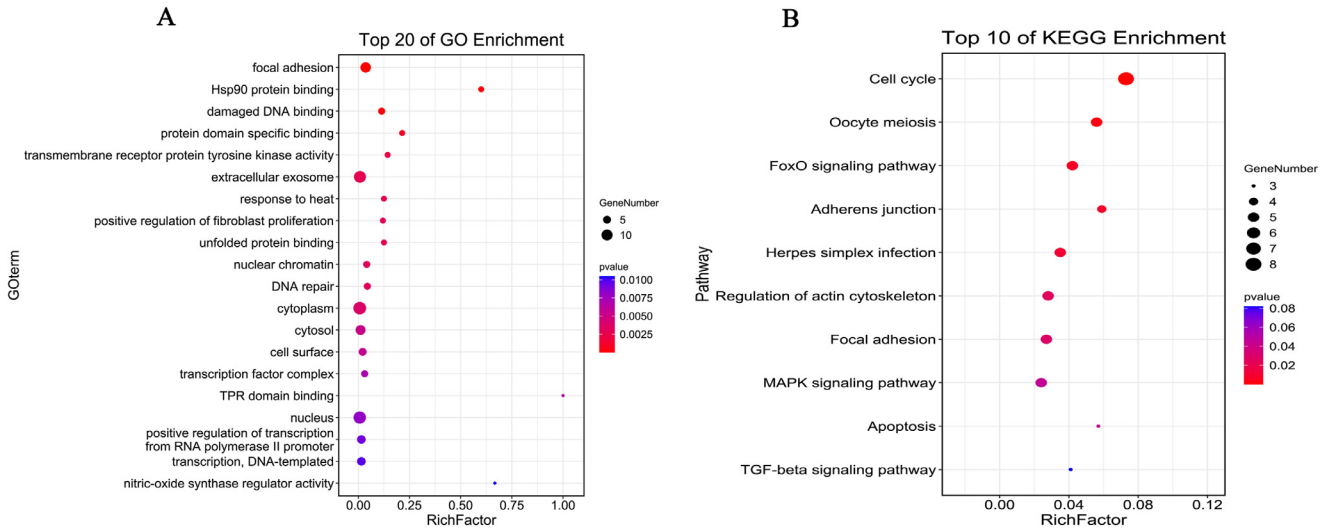

Figure 4. GO functional analysis and KEGG enrichment analysis. (A) GO functional analysis bubble diagram. (B) KEGG enrichment pathway bubble diagram. The Y axis represents the name of GO term or Pathway, the X axis represents the enrichment factor, the size of the bubble represents the number of genes belonging to this Goterm or Pathway in the target gene set, and the color of the bubble represents the significance of enrichment, that is, the size of the P value.

surface, pulmonary congestion and edema and other symptoms. On the other hand, compared to those from the model group, the broilers from the QLJP groups and the L-Arg group had better appetites, larger bodies, neater feathers, brighter red wattles, and normal skin color. After necropsy, there was no ascites in the abdominal cavity. The organs in the abdominal cavity were normal, but a small amount of pericardial effusion was seen in some cases. These results demonstrated that the establishment of the broiler AS animal model was successful and that QLJP improved the clinical necropsy phenotypes of broilers.

Effect of QLJP on Body Weight and the AHI of Broilers

The results in Figure 5A show that at 21, 28, and 35 d of age, the body weights of broilers in the model group were significantly lower than those of broilers in the control group ($P < 0.05$ or $P < 0.01$). At each time point, the body weights of broilers in the QLJP high-dose group were significantly higher than those of broilers in the model group ($P < 0.05$ or $P < 0.01$). At 21, 28 and 42 days of age, the body weights of broilers in the QLJP medium-dose group were significantly higher than those of broilers in the model group ($P < 0.05$ or $P < 0.01$). At 21 and 42 days of age, the body weights of broilers in the L-Arg group were significantly higher than those of broilers in the model group ($P < 0.01$).

The AHIs of the different treatment groups are shown in Figure 5B. The AHI of the model group was significantly higher than that of the control group at each time point ($P < 0.05$ or $P < 0.01$). The AHI of broilers in the QLJP high-dose group was significantly lower than that of broilers in the model group at each time point ($P < 0.05$ or $P < 0.01$). At 28, 35, and 42 d of age, the AHI of broilers in the QLJP medium-dose group was significantly lower than that of broilers in the model group ($P < 0.01$). At 35 and 42 d of age, the AHI of broilers in the QLJP low-dose group was much lower than that of broilers in the model group ($P < 0.01$). At 35 and 42 d of age, the AHI of broilers in the L-Arg group was significantly lower than that of broilers in the model group ($P < 0.01$). The above results indicate that QLJP increased the body weight of the broilers, significantly reduced the AHI of the broilers, and reduced the occurrence of AS in the broilers.

Protective Effect of QLJP against Lung Damage of Broilers

As shown in Figure 6, compared to the QLJP groups and the L-Arg group, the model group exhibited a significantly wider pulmonary interstitium, dilated alveoli and alveolar ducts, significantly thickened walls of pulmonary arterioles, later-stage alveolar wall thickening, atrophy of some of the alveoli, significant lumen narrowing, and coverage of the perivascular edema with a large number of inflammatory cells. These results suggest that QLJP protects broiler lungs from AS.

Effects of QLJP on Lung SOD, GPX, CAT, and MDA Levels

As shown in Figure 7A, at 21, 28, and 42 d of age, the SOD levels in the model group were significantly lower than those in the control group ($P < 0.05$ or $P < 0.01$). The SOD level of the QLJP high-dose group was significantly higher than that of the model group at each time point ($P < 0.05$ or $P < 0.01$). At 28, 35, and 42 d of age, the SOD levels of the QLJP medium-dose group were markedly higher than those of the model group ($P < 0.05$ or $P < 0.01$). At 28 and 42 d of age, the SOD levels of the L-Arg group were observably higher than those of the model group ($P < 0.01$).

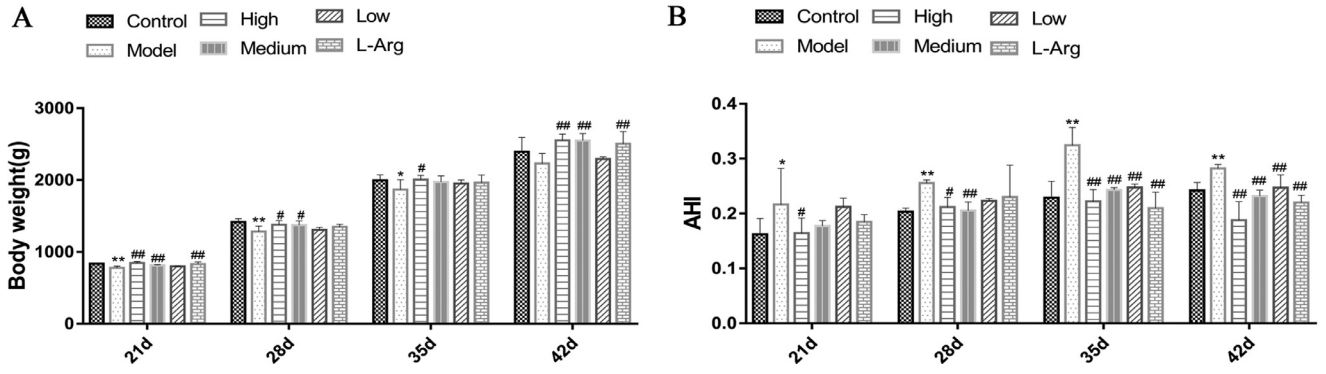

Figure 5. The effect of QLJP on body weight and the AHI of broilers. (A) Body weight of broilers. (B) The AHI values of broilers. Control: the control group, Model: the model group, High: the QLJP high-dose group, Medium: the QLJP medium-dose group, Low: the QLJP low-dose group, L-Arg: the L-arginine group. Data was noted as the mean ± SEM (n = 5). $^{*}P < 0.05$, $^{**}P < 0.01$, compared to the control group; $^{\#}P < 0.05$, $^{\#\#}P < 0.01$, compared to the model group.

Figure 7B shows that the GPX level of the model group was significantly lower than that of the control group at each time point ($P < 0.01$). The GPX levels of the QLJP high-dose and medium-dose groups were significantly higher than that of the model group at each time point ($P < 0.05$ or $P < 0.01$). At 28 d of age, the GPX level of the QLJP low-dose group was significantly higher than that of the model group ($P < 0.01$). The GPX level in the L-Arg group was significantly higher than that in the model group at each age ($P < 0.01$).

The CAT levels across the different groups are shown in Figure 7C. At 21, 35, and 42 d of age, the CAT levels of the model group were significantly lower than those of the control group ($P < 0.01$). At 21, 35, and 42 d of age, the CAT levels of the QLJP high-dose group and medium-dose group were significantly higher than those of the model group ($P < 0.05$ or $P < 0.01$). At 35 and 42 d of age, the CAT levels of the QLJP low-dose group were significantly higher than those of the model group ($P < 0.01$). At 21, 35, and 42 d of age, the CAT levels of the L-Arg group were significantly higher than those of the model group ($P < 0.01$).

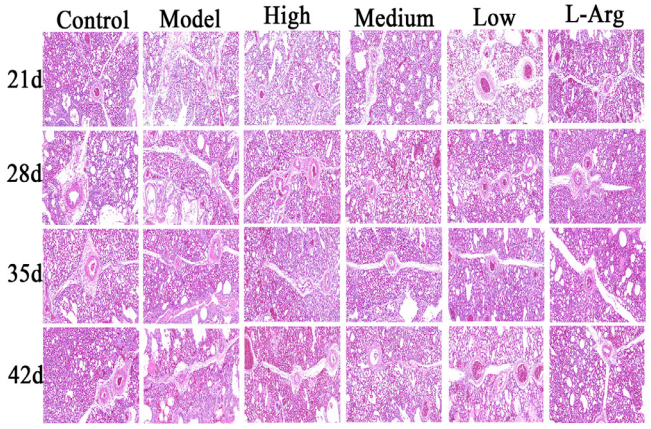

Figure 6. QLJP protect broiler lungs from AS damage. Histopathological observation of the lungs in different experimental groups at each time point. Control: the control group, Model: the model group, High: the QLJP high-dose group, Medium: the QLJP medium-dose group, Low: the QLJP low-dose group, L-Arg: the L-arginine group. H.E. stain (200 ×), scale bar =50 μm.

Figure 7D shows that at each time point, the MDA level in the model group was significantly higher than that in the control group ($P < 0.01$). The MDA level in each QLJP dose group was much lower than that in the model group at each time point ($P < 0.01$). The MDA level in the L-Arg group was much lower than that in the model group at each age ($P < 0.01$).

These results indicate that QLJP increased the levels of the antioxidant enzymes SOD, GPX, and CAT in the lungs of broilers, downregulated the level of MDA, and protected the lungs from oxidative stress damage.

Effects of QLJP on Lung Cell Apoptosis and Cell Cycle-related Gene mRNA Levels

As shown in Figure 8A, B, compared to those in the control group, the *FOXO3a* and *TP53* mRNA levels in the model group were extremely reduced at each time point ($P < 0.01$). Compared to those in the model group, the *FOXO3a* and *TP53* mRNA levels in the QLJP and L-Arg groups were extremely increased at each time point ($P < 0.01$).

The *BCL2, CDK2*, and *CCND1* mRNA levels across the different treatment groups are presented in Figure 8C-E. The *BCL2* mRNA level of the model group was much higher than that of the control group ($P < 0.01$), the *BCL2* mRNA level of each QLJP dose group was significantly lower than that of the model group at each time point ($P < 0.05$ or $P < 0.01$), and the *BCL2* mRNA level of the L-Arg group was much lower than that of the model group at each time point ($P < 0.01$). At each time point, the *CDK2* and *CCND1* mRNA levels of the model group were much higher than those of the control group ($P < 0.01$), the *CDK2* and *CCND1* mRNA levels of the QLJP groups were significantly lower than those of the model group ($P < 0.05$ or $P < 0.01$), and the *CDK2* and *CCND1* mRNA levels of the L-Arg group were much lower than those of the model group ($P < 0.01$).

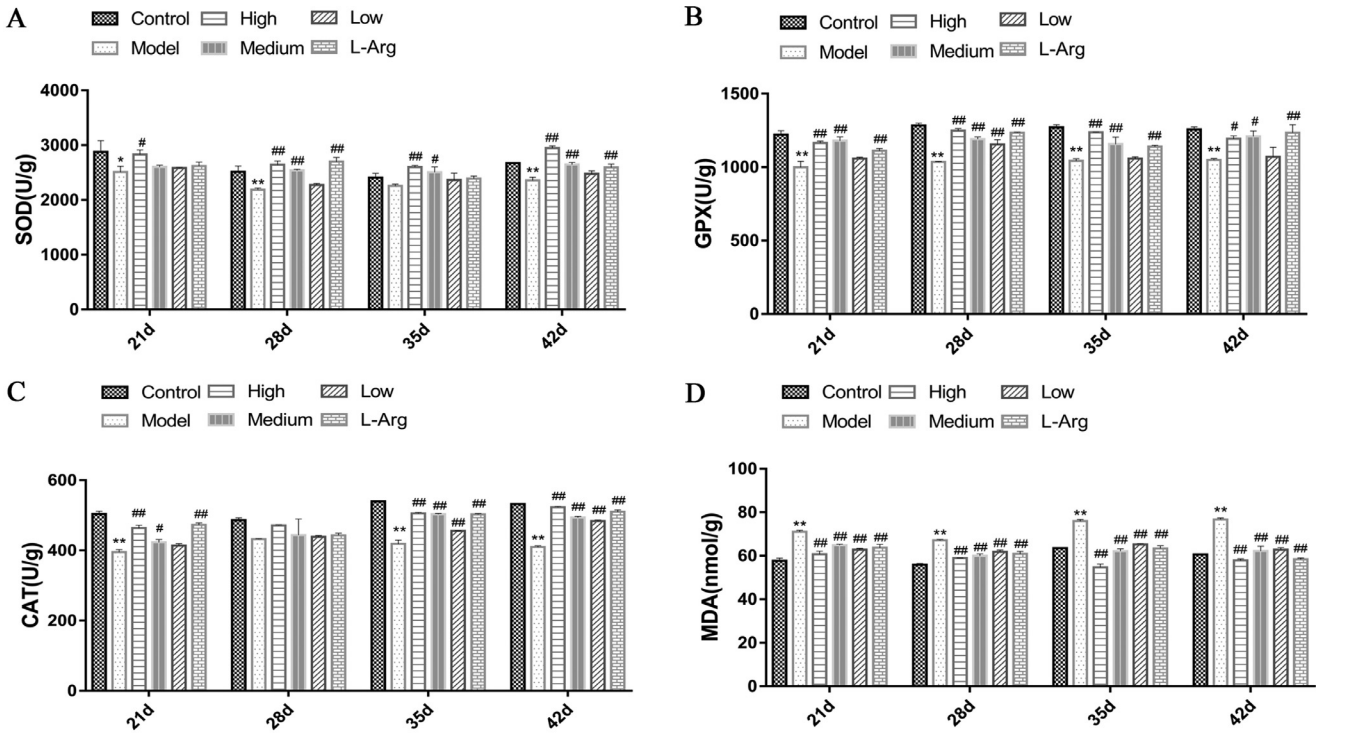

Figure 7. The effect of QLJP on lung SOD, GPX, CAT, and MDA levels. (A) SOD levels. (B) GPX levels. (C) CAT levels. (D) MDA levels. Control: the control group, Model: the model group, High: the QLJP high-dose group, Medium: the QLJP medium-dose group, Low: the QLJP low-dose group, L-Arg: the L-arginine group. Data was noted as the mean ± SEM (n = 5). $^{*}P < 0.05$, $^{**}P < 0.01$, compared to the control group; $^{\#}P < 0.05$, $^{\#\#}P < 0.01$, compared to the model group.

Effect of QLJP on the Expression of FOXO3a Protein in the Lungs

As shown in Figure 9, at 21 and 28 d of age, the FOXO3a protein expression level of the model group was lower than that of the control group ($P < 0.01$), and the FOXO3a protein expression levels of the QLJP groups were significantly higher than those of the model group at 21 and 28 d ($P < 0.05$ or $P < 0.01$). The FOXO3a protein expression levels in the QLJP high- and medium-dose groups at 35 and 42 d, and in the low-dose group at 42 d were significantly higher than those in the model group ($P < 0.05$ or $P < 0.01$). At each time point, the FOXO3a protein expression level in the L-Arg group was much higher than that in the model group ($P < 0.01$).

Effects of QLJP on the Protein Levels of TP53, BCL2, CDK2, and CCND1 in the Lungs

As shown in Figure 10A, at each time point, the TP53 protein level of the model group was significantly lower

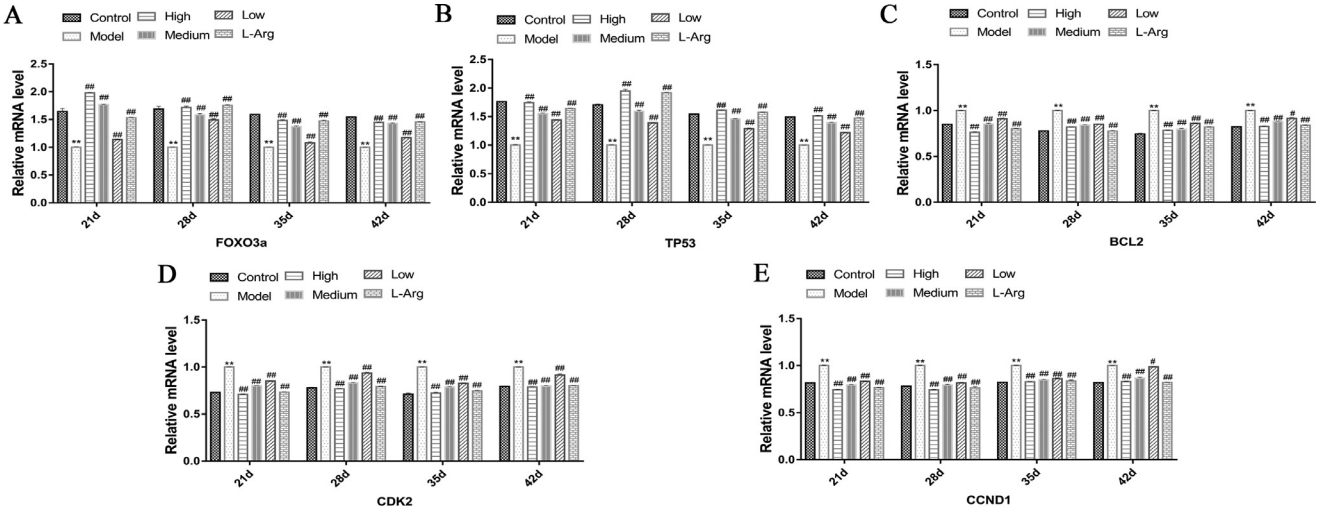

Figure 8. The effect of QLJP on lung cell apoptosis and cell cycle-related gene mRNA levels. (A) *FOXO3a* mRNA expression levels. (B) *TP53* mRNA expression levels. (C) *BCL2* mRNA expression levels. (D) *CDK2* mRNA expression levels. (E) *CCND1* mRNA expression levels. Control: the control group, Model: the model group, High: the QLJP high-dose group, Medium: the QLJP medium-dose group, Low: the QLJP low-dose group, L-Arg: the L-arginine group. Data was noted as the mean ± SEM (n = 5). $^{**}P < 0.01$, compared to the control group; $^{\#}P < 0.05$, $^{\#\#}P < 0.01$, compared to the model group.

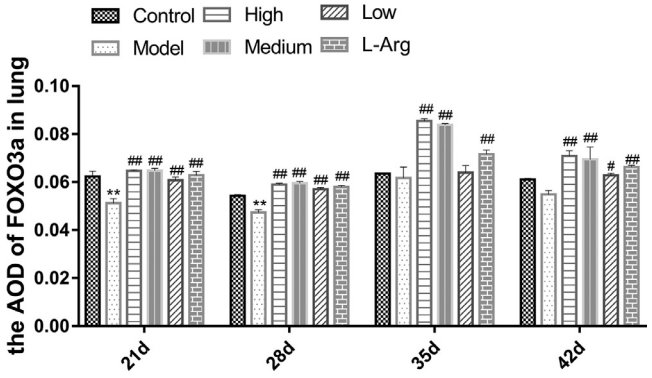

Figure 9. The effect of QLJP on the AOD of FOXO3a protein in lung. Control: the control group, Model: the model group, High: the QLJP high-dose group, Medium: the QLJP medium-dose group, Low: the QLJP low-dose group, L-Arg: the L-arginine group. Data was noted as the mean ± SEM (n = 10). $^{**}P < 0.01$, compared to the control group; $^{\#}P < 0.05$, $^{\#\#}P < 0.01$, compared to the model group.

than that of the control group ($P < 0.01$). Compared to the model group, the QLJP groups and the L-Arg group exhibited significantly higher TP53 protein levels at each time point, except for the QLJP low-dose group at 21 and 35 d ($P < 0.05$ or $P < 0.01$).

The BCL2 protein levels in the different groups are shown in Figure 10B. At each time point, the BCL2 protein level in the model group was much higher than that in the control group ($P < 0.01$). The BCL2 protein levels in the QLJP groups and the L-Arg group were significantly lower than that in the model group at each time point ($P < 0.05$ or $P < 0.01$).

Figure 10C-D shows that the CDK2 protein level was much higher in the model group than in the control group at each time point ($P < 0.01$). The CDK2 protein levels were much lower in the QLJP groups and the L-Arg group than those in the model group at each time point, except in the QLJP low-dose group at day 35 and the L-Arg group at day 21 ($P < 0.01$). At 21, 35, and 42 d of age, the CCND1 protein levels were much higher in the model group than in the control group ($P < 0.01$) and significantly lower in the QLJP high-dose group than in the model group ($P < 0.05$ or $P < 0.01$). Compared to those in the model group, the CCND1 protein levels in the QLJP medium-dose group on days 21 and 35 and the low-dose group on day 21 were significantly lower ($P < 0.05$ or $P < 0.01$). In addition, at 21 and 35 d of age, the CCND1 protein levels in the L-Arg group were significantly lower than those in the model group ($P < 0.05$).

DISCUSSION

Characteristics of modern broiler breeds such as their active metabolism, fast growth and high meat production have led to significant increases in the incidence of broiler AS and related mortality (Baghbanzadeh and Decuypere, 2008; Kalmar et al., 2013; Varmaghany et al., 2015). In order to maintain the best performance of broilers, it is very important to develop natural medicines or new feed additives to ameliorate AS. In recent years, the use of traditional Chinese medicine has gained increasing acceptance worldwide due to its multitarget and multilevel functional effects (Hu and Wang, 2019). Therefore, we investigated the mechanism of QLJP in the treatment of

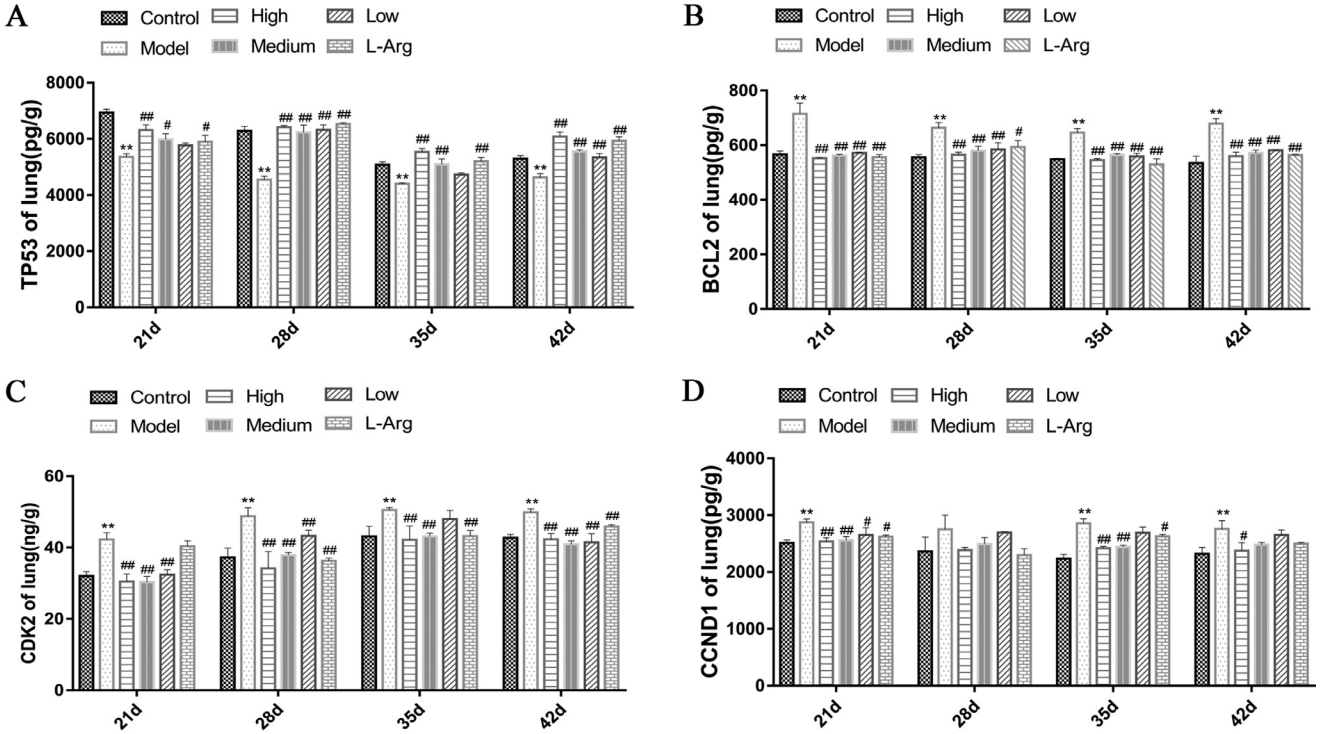

Figure 10. The effects of QLJP on the protein levels of TP53, BCL2, CDK2, and CCND1 in lung. Control: the control group, Model: the model group, High: the QLJP high-dose group, Medium: the QLJP medium-dose group, Low: the QLJP low-dose group, L-Arg: the L-arginine group. Data was noted as the mean ± SEM (n = 5). $^{**}P < 0.01$, compared to the control group; $^{\#}P < 0.05$, $^{\#\#}P < 0.01$, compared to the model group.

AS in broilers. Such research is of great significance for the prevention and treatment of AS in broilers.

In this study, in view of the complexity of the QLJP compounds and the diversity of the potential targets, we first screened the targets of the compounds in QLJP and broiler AS disease-related targets from multiple databases through network pharmacology. Then, a QLJP −single drug−compound−target network was constructed, and the main active compounds of QLJP were predicted, which were mainly from *Astragalus membranaceus* and *Gynostemma pentaphyllum*. Furthermore, the core targets of QLJP for the treatment of broiler AS were obtained through PPI network analysis. Our research revealed that the main active compounds of QLJP are primarily involved in the regulation of cell proliferation, the cell cycle, apoptosis, RNA polymerase II promoter transcription, and the hypoxia response. Hypoxia is the initiating factor of AS in broilers, causing tissue and cell damage with excess cell proliferation and resistance to apoptosis (Moudgil et al., 2006; Wang et al., 2007). It leads to pulmonary dysfunction, pulmonary vascular remodeling, and PAH. These results suggest a molecular mechanism in which QLJP regulates oxidative stress, cell proliferation and apoptosis to interfere with AS in broilers.

Previous studies have reported that AS broilers exhibit significant weight loss, damage to all organs, and a significantly increased AHI. Dynamic changes in the AHI reflect the development process of AS (Wideman, 2001), and lung damage might trigger AS (Julian, 2000). Similarly, in our study, the broilers in the model group had significantly decreased body weights, histological damage to the lungs, and significantly increased AHI values. Previous research has shown that this impairment can be alleviated by dietary vitamin C, flax oil and antioxidants (Walton et al., 2001; Villar et al., 2002). Our results indicate that QLJP can attenuate the clinical symptoms of broilers, increase broiler weight, ameliorate histological damage, improve lung function, and significantly reduce the AHI in broilers. Other studies have also revealed that the addition of compounds that inactivate or remove reactive oxygen species (**ROS**) and H_2O_2 can reduce the oxidative stress damage caused by AS in broilers (Cruz et al., 2003). In addition, erythrocyte antioxidants protect other tissues, particularly the lungs, against tissue damage produced by ROS (Heffner and Repine, 1989). Our research showed that QLJP increased the levels of the antioxidant enzymes SOD, GPX, and CAT and reduced the content of MDA in the lungs from the levels in the model group. Similarly, other studies have shown that the addition of alpha-tocopherol increases the levels of antioxidant enzymes in broilers and reduces lipid oxidative damage, suggesting that a reduction in oxidative stress is associated with a reduction in AS mortality (Bottje et al., 1995). These findings demonstrate that QLJP exerts important effects to protect broilers and interfere with AS.

Our enrichment analysis indicated that the core targets might be mainly associated with the FOXO signaling pathway, Cell cycle, Adherens junctions, Focal adhesion, MAPK signaling pathway, Apoptosis, and TGF-β signaling pathway. According to previous reports, FOXOs are involved in regulating host responses to various stresses (such as hypoxia and DNA damage), and their downstream signals regulate multiple processes, such as oxidative stress, apoptosis and cell cycle arrest (Paik, 2006; Eijkelenboom and Burgering, 2013). In addition, FOXO3a has been shown to play important roles in various biological processes, including development, proliferation, apoptosis, metabolism, and differentiation, by regulating a broad spectrum of genes (Abid et al., 2005; Lee et al., 2007, 2008). In our study, the FOXO3a mRNA and protein levels were lower in the model group than in the control group at each time point. Consistent with our findings, the findings of Zhao et al. (2019) suggest that the expression level of FOXO3a is reduced under hypoxic conditions. However, the FOXO3a mRNA and protein levels were higher in the QLJP groups than those in the model group at each time point. Notably, according to the available literature, FOXO3a is a core regulator of cellular homeostasis and the stress response (Abid et al., 2005), and in a rat carotid artery balloon injury model, activated FOXO3a has been found to inhibit the proliferation of VSMCs to improve vascular function (Fasano et al., 2019). Other studies have also shown that FOXO3a can lead to stabilization and activation of the p53 protein to induce cell cycle arrest and apoptosis (You et al., 2006; Wang et al., 2008). The results of our study showed that QLJP increased the expression level of TP53 and decreased the expression levels of BCL2, CDK2, and CCND1 compared to the levels in the model group at each time point. Therefore, we speculate that QLJP induces cell cycle arrest and apoptosis via the FOXO3a signaling pathway. Studies have proven that pulmonary artery remodeling is a key step in the development of AS, also known as PAH (Yang et al., 2016). Furthermore, it has been revealed that the pathologic features of pulmonary artery remodeling are attributable to an increase in proliferation and a decrease in apoptosis of pulmonary VSMCs and endothelial cells (Mandegar et al., 2002). Our results also demonstrate that QLJP might inhibit pulmonary cell proliferation and pulmonary vascular remodeling by regulating the FOXO3a signaling pathway, reducing PAH, and reducing the occurrence and development of AS in broilers.

CONCLUSION

In this study, we investigated the active compounds of QLJP in the treatment of broiler AS and their underlying mechanisms of action through network pharmacology. We obtained 49 active compounds, of which the main active compounds were quercetin, kaempferol, hederagenin, 7-O-methylisomucronulatol, formononetin, and isorhamnetin, etc. Further KEGG enrichment analysis of QLJP treatment for broiler AS revealed 35 signaling pathways, and the key mechanism was mainly related to the FOXO signaling pathway, cell cycle,

apoptosis, and oxidative stress. In animal experiments, the clinical and anatomical symptoms of broilers in the model group were consistent with the previously reported characteristics of AS broilers. The body weights of the broilers were significantly reduced, and the AHI values were significantly increased. QLJP exerted a protective effect on AS broilers by improving the clinical symptoms and lung function, increasing the body weight, and reducing the AHI values of the broilers. In addition, we identified the potential mechanisms underlying the protective functions of QLJP in AS broilers. QLJP may increase the ability of broilers to resist oxidative stress, block cell cycle progression, induce cell apoptosis, inhibit cell proliferation, reduce PAH, and subsequently reduce the occurrence and development of AS in broilers by activating the FOXO3a signaling pathway. This study, for the first time, established a scientific basis for the clinical effects of QLJP in the treatment of broiler AS through network pharmacological analysis and animal experimental research, and the findings lay a solid foundation for further elucidation of the effective components and mechanisms of QLJP in the treatment of broiler AS.

ACKNOWLEDGMENTS

This work was supported by the Natural Science Foundation of Shanxi Province (Grant No.201901D111235), and the Modern agricultural industrial technology system of Henan Province (Grant No.S2012-06-G02).

DISCLOSURES

The authors declare that there is no conflict of interest.

SUPPLEMENTARY MATERIALS

Supplementary material associated with this article can be found in the online version at doi:10.1016/j.psj.2022.102144.

REFERENCES

Abid, M. R., K. Yano, S. Guo, V. I. Patel, G. Shrikhande, K. C. Spokes, C. Ferran, and W. C. Aird. 2005. Forkhead transcription factors inhibit vascular smooth muscle cell proliferation and neointimal hyperplasia. J. Biol. Chem. 280:29864–29873.

Ahmadipour, B., M. Sharifi, and F. Khajali. 2018. Pulmonary hypertensive response of broiler chickens to arginine and guanidinoacetic acid under high-altitude hypoxia. Acta. Vet. Hung. 66:116–124.

Baghbanzadeh, A., and E. Decuypere. 2008. Ascites syndrome in broilers: physiological and nutritional perspectives. Avian Pathol. 37:117–126.

Bordenave, J., L. Tu, L. Savale, A. Huertas, M. Humbert, and C. Guignabert. 2019. New insights in the pathogenesis of pulmonary arterial hypertension. Rev. Mal. Respir. 36:433–437.

Bottje, W., B. Enkvetchakul, R. Moore, and R. McNew. 1995. Effect of alpha-tocopherol on antioxidants, lipid peroxidation, and the incidence of pulmonary hypertension syndrome (ascites) in broilers. Poult. Sci. 74:1356–1369.

Brown, A. K., and A. E. Webb. 2018. Regulation of FOXO factors in mammalian cells. Curr. Top. Dev. Biol. 127:165–192.

Cheng, T. C., J. F. Lu, J. S. Wang, L. J. Lin, H. I. Kuo, and B. H. Chen. 2011. Antiproliferation effect and apoptosis mechanism of prostate cancer cell PC-3 by flavonoids and saponins prepared from Gynostemma pentaphyllum. J. Agric. Food. Chem. 59:11319–11329.

Chinese Veterinary Pharmacopoeia Committee. 2017. Quality standards for veterinary drugs: Traditional Chinese Medicine Volume: *2017*China Agriculture Press, Beijing, 146–147.

Chung, H. W., J. H. Lim, M. Y. Kim, S. J. Shin, S. Chung, B. S. Choi, H. W. Kim, Y. S. Kim, C. W. Park, and Y. S. Chang. 2012. High-fat diet-induced renal cell apoptosis and oxidative stress in spontaneously hypertensive rat are ameliorated by fenofibrate through the PPARa-FOXO3aa-PGC-1a pathway. Nephrol. Dial. Transplant. 27:2213–2225.

Courboulin, A., M. Barrier, T. Perreault, P. Bonnet, V. L. Tremblay, R. Paulin, E. Tremblay, C. Lambert, M. H. Jacob, S. N. Bonnet, S. Provencher, and S. Bonnet. 2012. Plumbagin reverses proliferation and resistance to apoptosis in experimental PAH. Eur. Respir. J. 40:618–629.

Dai, B. S., C. B. Su, and S. X. Chen. 2007. Research advances on prevention and cure effects of Chinese Herbal Medicine against broiler ascites syndrome. J. Anhui Agri. Sci. 35:3874–3876.

Díaz-Cruz, A., M. Serret, G. Ramírez, E. Avila, R. Guinzberg, and E. Piña. 2003. Prophylactic action of lipoic acid on oxidative stress and growth performance in broilers at risk of developing ascites syndrome. Avian Pathol. 32:645–653.

Eijkelenboom, A., and B. M. Burgering. 2013. FOXOs: signalling integrators for homeostasis maintenance. Nat. Rev. Mol. Cell. Biol. 14:83–97.

Fasano, C., V. Disciglio, S. Bertora, M. Lepore-Signorile, and C. Simone. 2019. FOXO3a from the nucleus to the mitochondria: a round trip in cellular stress response. Cells. 8:1110.

Feng, L., T. T. Liu, X. K. Huo, X. G. Tian, C. Wang, X. Lv, J. Ning, W. Y. Zhao, B. J. Zhang, C. P. Sun, and X. C. Ma. 2021. Alisma genus: phytochemical constituents, biosynthesis, and biological activities. Phytother. Res. 35:1872–1886.

Fu, J., Z. Wang, L. Huang, S. Zheng, D. Wang, S. Chen, H. Zhang, and S. Yang. 2014. Review of the botanical characteristics, phytochemistry, and pharmacology of Astragalus membranaceus (Huangqi). Phytother. Res. 28:1275–1283.

Heffner, J. E., and J. E. Repine. 1989. Pulmonary strategies of antioxidant defense. Am. Rev. Respir. Dis. 140:531–554.

Humbert, M., N. W. Morrell, S. L. Archer, K. R. Stenmark, M. R. MacLean, I. M. Lang, B. W. Christman, E. K. Weir, O. Eickelberg, N. F. Voelkel, and M. Rabinovitch. 2004. Cellular and molecular pathobiology of pulmonary arterial hypertension. J. Am. Coll. Cardiol. 43(12 Suppl S):13S–24S.

Hu, Y. W., C. Y. Liu, C. M. Du, J. Zhang, W. Q. Wu, and Z. L. Gu. 2009. Induction of apoptosis in human hepatocarcinoma SMMC-7721 cells in vitro by flavonoids from Astragalus complanatus. J. Ethnopharmacol. 123:293–301.

Hu, Y., and J. Wang. 2019. Interactions between clopidogrel and traditional Chinese medicine. J. Thromb. Thrombol. 48:491–499.

Julian, R. J. 1987. The effect of increased sodium in the drinking water on right ventricular failure and ascites in broiler chickens. Avian Pathol. 16:61–71.

Julian, R. J., I. McMillan, and M. Quinton. 1989. The effect of cold and dietary energy on right ventricular hypertrophy, right ventricular failure and ascites in meat-type chickens. Avian Pathol. 18:675–684.

Julian, R. J. 1993. Ascites in poultry. Avian Pathol. 22:419–454.

Julian, R. J. 2000. Physiological, management and environmental triggers of the ascites syndrome: a review. Avian Pathol. 29:519–527.

Kalmar, I. D., D. Vanrompay, and G. P. Janssens. 2013. Broiler ascites syndrome: collateral damage from efficient feed to meat conversion. Vet. J. 197:169–174.

Lee, H. Y., J. W. Chung, S. W. Youn, J. Y. Kim, K. W. Park, B. K. Koo, B. H. Oh, Y. B. Park, B. Chaqour, K. Walsh, and H. S. Kim. 2007. Forkhead transcription factor FOXO3a is a negative regulator of angiogenic immediate early gene CYR61, leading to inhibition of vascular smooth muscle cell proliferation and neointimal hyperplasia. Circ. Res. 100:372–380.

Lee, H. Y., H. J. You, J. Y. Won, S. W. Youn, H. J. Cho, K. W. Park, W. Y. Park, J. S. Seo, Y. B. Park, K. Walsh, B. H. Oh, and

H. S. Kim. 2008. Forkhead factor, FOXO3a, induces apoptosis of endothelial cells through activation of matrix metalloproteinases. Arterioscler. Thromb. Vasc. Biol. 28:302–308.

Li, J., W. Du, S. Maynard, P. R. Andreassen, and Q. Pang. 2010. Oxidative stress-specific interaction between FANCD2 and FOXO3a. Blood. 115:1545–1548.

Li, B., X. Y. Zhang, M. Z. Wang, and L. L. Jiao. 2015. Characterization and antioxidant activities of acidic polysaccharides from Gynostemma pentaphyllum (Thunb.) Markino. Carbohydr Polym. 127:209–214.

Liu, Y. F., N. Ai, A. Keys, X. H. Fan, and M. J. Chen. 2015. Network Pharmacology for traditional Chinese medicine research: Methodologies and applications. Chin. Herb. Med. 7:18–26.

Mandegar, M., C. V. Remillard, and J. X. Yuan. 2002. Ion channels in pulmonary arterial hypertension. Prog. Cardiovasc. Dis. 45:81–114.

Moudgil, R., E. D. Michelakis, and S. L. Archer. 2006. The role of k^+ channels in determining pulmonary vascular tone, oxygen sensing, cell proliferation, and apoptosis: implications in hypoxic pulmonary vasoconstriction and pulmonary arterial hypertension. Microcirculation. 13:615–632.

Paik, J. H 2006. FOXOs in the maintenance of vascular homoeostasis. Biochem. Soc. Trans. 34(Pt 5):731–734.

Papanicolaou, K. N., Y. Izumiya, and K. Walsh. 2008. Forkhead transcription factors and cardiovascular biology. Circ. Res. 102:16–31.

Qi, Y. H., and W. K. Wang. 2006. The effect of Zhenwu decoction on prevention and treatment of broiler ascites syndrome. Anim. Husbandry Vet. Med. 38:15–17.

Reiterer, M., and S. L. Milton. 2020. Induction of foxo3a protects turtle neurons against oxidative stress. Comp. Biochem. Physiol. A Mol. Integr. Physiol. 243:110671.

Ríos, J. L. 2011. Chemical constituents and pharmacological properties of Poria cocos. Planta Med. 77:681–691.

Shi, Y. X., D. M. Lin, Y. Y. Zhang, and Q. M. Bao. 2005. Effect of Herb Medicines on the proportion of moisture free tissue weight of broiler ascites syndrom. China Poultry. 27:15–16.

Stenmark, K. R., K. A. Fagan, and M. G. Frid. 2006. Hypoxia-induced pulmonary vascular remodeling: cellular and molecular mechanisms. Circ. Res. 99:675–691.

Tia, N., A. K. Singh, P. Pandey, C. S. Azad, P. Chaudhary, and I. S. Gambhir. 2018. Role of Forkhead Box O (FOXO) transcription factor in aging and diseases. Gene. 648:97–105.

Tsui, K. C., T. H. Chiang, J. S. Wang, L. J. Lin, W. C. Chao, B. H. Chen, and J. F. Lu. 2014. Flavonoids from Gynostemma pentaphyllum exhibit differential induction of cell cycle arrest in H460 and A549 cancer cells. Molecules. 19:17663–17681.

Tuder, R. M., J. H. Yun, A. Bhunia, and I. Fijalkowska. 2007. Hypoxia and chronic lung disease. J. Mol. Med. (Berl). 85:1317–1324.

Varmaghany, S., M. A. Karimi-Torshizi, S. Rahimi, H. Lotfollahian, and M. Hassanzadeh. 2015. The effects of increasing levels of dietary garlic bulb on growth performance, systolic blood pressure, hematology, and ascites syndrome in broiler chickens. Poult. Sci. 94:1812–1820.

Villar-Patiño, G., A. Díaz-Cruz, E. Avila-González, R. Guinzberg, J. L. Pablos, and E. Piña. 2002. Effects of dietary supplementation with vitamin C or vitamin E on cardiac lipid peroxidation and growth performance in broilers at risk of developing ascites syndrome. Am. J. Vet. Res. 63:673–676.

Walton, J. P., R. J. Julian, and E. J. Squires. 2001. The effects of dietary flax oil and antioxidants on ascites and pulmonary hypertension in broilers using a low temperature model. Br Poult. Sci. 42:123–129.

Wang, J., J. Qiao, L. H. Zhao, K. Li, H. Wang, T. Xu, Y. Tian, M. Gao, and X. Wang. 2007. Proliferation of pulmonary artery smooth muscle cells in the development of ascites syndrome in broilers induced by low ambient temperature. J. Vet. Med. A. Physiol. Pathol. Clin. Med. 54:564–570.

Wang, Q. F., C. W. Chiang, C. C. Wu, C. C. Cheng, S. J. Hsieh, J. C. Chen, Y. C. Hsieh, and S. L. Hsu. 2007. Gypenosides induce apoptosis in human hepatoma Huh-7 cells through a calcium/reactive oxygen species-dependent mitochondrial pathway. Planta Med. 73:535–544.

Wang, F., C. B. Marshall, K. Yamamoto, G. Y. Li, M. J. Plevin, H. You, T. W. Mak, and M. Ikura. 2008. Biochemical and structural characterization of an intramolecular interaction in FOXO3a and its binding with p53. J. Mol. Biol. 384:590–603.

Wang, Z., T. Yu, and P. Huang. 2016. Post-translational modifications of FOXO family proteins. Mol. Med. Rep. 14:4931–4941.

Wang, J., H. Li, T. Xia, J. Feng, and R. Zhou. 2021. Pulmonary arterial hypertension and flavonoids: a role in treatment. Chin. J. Physiol. 64:115–124.

Wei, W., X. M. Zhou, Y. C. Wang, Z. C. Lin, and J. H. Xue. 2018. Effect of alisol A 24-acetate on proliferation of aorta smooth muscle cells in rats induced by ox-LDL. Zhongguo Zhong Yao Za Zhi. 43:2147–2152.

Wideman, R. F. 2001. Pathophysiology of heart/lung disorders:Pulmonary hypertension syndrome in broiler chickens. World's. Poult. Sci. J. 57:289–307.

Wideman, R. F., K. R. Hamal, M. T. Bayona, A. G. Lorenzoni, D. Cross, and F. Khajali. 2011. Plexiform lesions in the lungs of domestic fowl selected for susceptibility to pulmonary arterial hypertension: incidence and histology. Anat. Rec. 294:739–755.

Wideman, R. F., D. D. Rhoads, G. F. Erf, and N. B. Anthony. 2013. Pulmonary arterial hypertension (ascites syndrome) in broilers. A review. Poult. Sci. 92:64–83.

Xu, Q., R. Bauer, B. M. Hendry, T. P. Fan, Z. Zhao, P. Duez, M. S. Simmonds, C. M. Witt, A. Lu, N. Robinson, D. A. Guo, and P. J. Hylands. 2013. The quest for modernisation of traditional Chinese medicine. BMC Complement. Altern. Med. 13:132.

Yang, F., H. Cao, Q. Xiao, X. Guo, Y. Zhuang, C. Zhang, T. Wang, H. Lin, Y. Song, G. Hu, and P. Liu. 2016. Transcriptome analysis and gene identification in the pulmonary artery of broilers with Ascites Syndrome. PLoS One. 11:e0156045.

You, H., K. Yamamoto, and T. W. Mak. 2006. Regulation of transactivation-independent proapoptotic activity of p53 by FOXO3a. Proc. Natl. Acad. Sci. U S A. 103:9051–9056.

Yuan, H., Q. Ma, H. Cui, G. Liu, X. Zhao, W. Li, and G. Piao. 2017. How can synergism of traditional medicines benefit from network pharmacology? Molecules. 22:1135.

Zhang, Z. Q., X. C. Cao, and L. Zhang. 2005. Effect of shikonin on rat vascular smooth muscle cells proliferation and apoptosis in vitro. Natl. Med. J. China. 85:1484–1488.

Zhang, X. S., C. Zhao, W. Z. Tang, X. J. Wu, and Y. Q. Zhao. 2015. Gypensapogenin H, a novel dammarane-type triterpene induces cell cycle arrest and apoptosis on prostate cancer cells. Steroids. 104:276–283.

Zhang, R., X. Zhu, H. Bai, and K. Ning. 2019. Network pharmacology databases for traditional chinese medicine: review and assessment. Front. Pharmacol. 10:123.

Zhao, M., N. Chen, X. Li, and L. Lin. 2019. MiR-629 regulates hypoxic pulmonary vascular remodelling by targeting FOXO3 and PERP. J. Cell. Mol. Med. 23:5165–5175.

Zhao, J., X. Niu, J. Yu, X. Xiao, W. Li, L. Zang, Z. Hu, Ip. P. Siu-Po, and W. Li. 2020. Poria cocos polysaccharides attenuated ox-LDL-induced inflammation and oxidative stress via ERK activated Nrf2/HO-1 signaling pathway and inhibited foam cell formation in VSMCs. Int. Immunopharmacol. 80:106173.